Newtonian heating effects in three-dimensional flow of viscoelastic fluid*

A. Qayyum[a)†], T. Hayat[a)b)], M. S. Alhuthali[b)], and H. M. Malaikah[b)]

[a)] *Department of Mathematics, Quaid-i-Azam University* 45320, *Islamabad* 44000, *Pakistan*

[b)] *Department of Mathematics, Faculty of Science, King Abdulaziz University, Jeddah* 21589, *Saudi Arabia*

(Received 17 July 2013; revised manuscript received 22 October 2013; published online 1 April 2014)

A mathematical model is constructed to investigate the three-dimensional flow of a non-Newtonian fluid. An incompressible viscoelastic fluid is used in mathematical formulation. The conjugate convective process (in which heat the transfer rate from the bounding surface with a finite capacity is proportional to the local surface temperature) in three-dimensional flow of a differential type of non-Newtonian fluid is analyzed for the first time. Series solutions for the nonlinear differential system are computed. Plots are presented for the description of emerging parameters entering into the problem. It is observed that the conjugate heating phenomenon causes an appreciable increase in the temperature at the stretching wall.

Keywords: viscoelastic fluid, three-dimensional flow, Newtonian heating

PACS: 47.50.Gj, 44.20.+b **DOI:** 10.1088/1674-1056/23/5/054703

1. Introduction

Viscoelastic materials are encountered in chemical engineering, physiology and nuclear industry. Mostly such materials have shear rate viscosity but some materials of this class have shear-independent viscosity. Examples of these materials include molten polymers, ketchup, toothpaste, custard, paints, shampoo, drilling mud, synovial fluid, whipped cream, syrup, jams, blood at a low shear rate and many others. The well-known Navier–Stokes equations can only characterize the shear properties of viscous fluid. These equations are inadequate for the characteristics of non-Newtonian fluids. Generally, the equations corresponding to non-Newtonian fluids are more complex, higher order and nonlinear than the Navier–Stokes equations. To compute analytic/numerical solutions to such equations is not an easy task. Many researchers in the past have discussed the steady and the unsteady flows of non-Newtonian fluids using different constitutive relationships. Some current studies on the topic may be directed to the attempts.[1–16]

The boundary layer flows generated by a stretching sheet are very important in aerodynamic extrusion of plastic sheet, metallurgy, nuclear reactors, glass fiber production, paper production, crystal growing, manufacture of foods, continuous casting, etc. After the pioneering work of Crane,[17] the boundary layer flows are extensively discussed (see Refs. [18]–[21] and the references therein). However, the previous available information on the topic shows that in most studies, the case of a two-dimensional stretched flow is taken care off. Limited attention is given to the three-dimensional stretched flow.[22–24] Such analysis further narrowed down when three-dimensional boundary layer flows subject to Newtonian heating[25] are considered. In Ref. [25], the author has proposed four methods for heating, namely, (i) constant wall temperature, (ii) constant surface heat flux, (iii) conjugate conductions, and (iv) Newtonian heating.

Traditionally, the heat transfer in boundary layer flows has been examined either through a prescribed surface temperature or heat flux. Here the objective of the present investigation is to model the three-dimensional flow of non-Newtonian fluid over a stretched surface with Newtonian heating effects. Viscoelastic fluid is employed in the mathematical formulation. This paper is organized as follows. The next section contains the problem statement and series solutions by the homotopy analysis method.[26–35] Discussion of various plots is presented in section three. Section four contains the concluding remarks.

2. Mathematical formulation

Lets us consider a steady three-dimensional flow of an incompressible viscoelastic fluid. The sheet is stretched bidirectionally in a linear manner located at $z = 0$. The heat transport phenomenon is taken into account in the presence of Newtonian heating (conjugate heating process). The laws of conservations of mass, momentum and energy equations for the present boundary layer flow take the following forms:

$$\frac{\partial u}{\partial x}+\frac{\partial v}{\partial y}+\frac{\partial w}{\partial z}=0, \tag{1}$$

$$u\frac{\partial u}{\partial x}+v\frac{\partial u}{\partial y}+w\frac{\partial u}{\partial z}$$

*Project supported by the Deanship of Scientific Research (DSR), King Abdulaziz University, Jeddah (Grant No. 10-130/1434HiCi).

†Corresponding author. E-mail: abq_bw76@yahoo.com

© 2014 Chinese Physical Society and IOP Publishing Ltd

$$= \nu\frac{\partial^2 u}{\partial z^2} - k\left[u\frac{\partial^3 u}{\partial x\partial z^2} + w\frac{\partial^3 u}{\partial z^3} - \left(\frac{\partial u}{\partial x}\frac{\partial^2 u}{\partial z^2} + \frac{\partial u}{\partial z}\frac{\partial^2 w}{\partial z^2} + 2\frac{\partial u}{\partial z}\frac{\partial^2 u}{\partial x\partial z} + 2\frac{\partial w}{\partial z}\frac{\partial^2 u}{\partial z^2}\right)\right], \quad (2)$$

$$u\frac{\partial v}{\partial x} + v\frac{\partial v}{\partial y} + w\frac{\partial v}{\partial z} = \nu\frac{\partial^2 v}{\partial z^2} - k\left[v\frac{\partial^3 v}{\partial y\partial z^2} + w\frac{\partial^3 v}{\partial z^3} - \left(\frac{\partial v}{\partial y}\frac{\partial^2 v}{\partial z^2} + \frac{\partial u}{\partial z}\frac{\partial^2 w}{\partial z^2} + 2\frac{\partial v}{\partial z}\frac{\partial^2 v}{\partial y\partial z} + 2\frac{\partial w}{\partial z}\frac{\partial^2 v}{\partial z^2}\right)\right], \quad (3)$$

$$u\frac{\partial T}{\partial x} + v\frac{\partial T}{\partial y} + w\frac{\partial T}{\partial z} = \alpha_{\mathrm{m}}\frac{\partial^2 T}{\partial z^2}, \quad (4)$$

where u, v, and w are the velocities in the x, y, and z directions, respectively, ν is the kinematic viscosity, k is the material parameter of fluid, T is the temperature, and α_{m} is the thermal diffusivity.

The boundary conditions for the present study can be written as

$$\begin{aligned} &u = u_{\mathrm{w}}(x) = ax,\ v = v_{\mathrm{w}}(y) = by,\\ &w = 0,\ \frac{\partial T}{\partial z} = -h_s T, \quad \text{at} \quad z = 0,\\ &u \to 0,\ v \to 0,\ \frac{\partial u}{\partial z} \to 0,\ \frac{\partial v}{\partial z} \to 0,\\ &T \to T_\infty, \quad \text{as} \quad z \to \infty, \end{aligned} \quad (5)$$

where $u = ax$ and $v = by$ are the stretching velocities along the x axis and the y axis, respectively, h_{s} is the heat transfer coefficient, and T_∞ is the temperature far away from the surface.

Setting

$$\begin{aligned} &\eta = \sqrt{\frac{a}{\nu}}z,\ u = axf'(\eta),\ v = ayg'(\eta),\\ &w = -\sqrt{a\nu}\ \{f(\eta) + g(\eta)\},\\ &\theta(\eta) = \frac{T - T_\infty}{T_\infty}, \end{aligned} \quad (6)$$

the continuity Eq. (1) is clearly satisfied and Eqs. (2)–(5) are transformed as follows:

$$f''' - f'^2 + (f+g)f'' + K_0\left[(f+g)f^{(iv)} + (f'' - g'')f'' - 2(f' + g')f'''\right] = 0, \quad (7)$$

$$g''' - g'^2 + (f+g)g'' + K_0\left[(f+g)g^{(iv)} + (g'' - f'')g'' - 2(f' + g')g'''\right] = 0, \quad (8)$$

$$\theta'' + Pr\,(f+g)\,\theta' = 0, \quad (9)$$

$$\begin{aligned} &f(0) = 0, \quad g(0) = 0, \quad f'(0) = 1, \quad g'(0) = c,\\ &\theta'(0) = -\gamma[1 + \theta(0)],\\ &f'(\infty) = 0, \quad g'(\infty) = 0, \quad f''(\infty) = 0,\\ &g''(\infty) = 0,\ \theta(\infty) \to 0, \end{aligned} \quad (10)$$

where the viscoelastic parameter K_0, the ratio parameter c, the conjugate parameter for Newtonian heating γ and Prandtl number Pr are defined by

$$\begin{aligned} &K_0 = ka/\nu,\ c = b/a,\ \gamma = \sqrt{\frac{\nu}{a}}h_{\mathrm{s}},\\ &Pr = \nu/\alpha_{\mathrm{m}}. \end{aligned} \quad (11)$$

Note that the two-dimensional ($g = 0$) case has been obtained for $c = 0$. Further, the axisymmetric situation is recovered when $f = g$.

An expression of the local Nusselt number is given by

$$Nu = \frac{xq_{\mathrm{w}}}{k(T - T_\infty)}, \quad (12)$$

subject to the value of q_{w} mentioned below

$$q_{\mathrm{w}} = -k\left(\frac{\partial T}{\partial z}\right)_{z=0}, \quad (13)$$

where q_{w} denotes the heat flux.

Equation (12) in dimensionless form becomes

$$Nu_x/Re_x^{1/2} = \gamma\left[1 + \frac{1}{\theta(0)}\right], \quad (14)$$

where $Re_x = u_{\mathrm{w}}x/\nu$ is the local Reynolds number.

3. Solutions

We choose the initial guesses

$$\begin{aligned} &f_0(\eta) = 1 - \mathrm{e}^{-\eta}, \quad g_0(\eta) = c\left(1 - \mathrm{e}^{-\eta}\right),\\ &\theta_0(\eta) = \frac{\gamma}{1-\gamma}\mathrm{e}^{-\eta}, \end{aligned} \quad (15)$$

and the linear operators

$$\begin{aligned} &\mathcal{L}_{\mathrm{f}} = \frac{\mathrm{d}^3}{\mathrm{d}\eta^3} - \frac{\mathrm{d}}{\mathrm{d}\eta}, \quad \mathcal{L}_{\mathrm{g}} = \frac{\mathrm{d}^3}{\mathrm{d}\eta^3} - \frac{\mathrm{d}}{\mathrm{d}\eta},\\ &\mathcal{L}_\theta = \frac{\mathrm{d}^2}{\mathrm{d}\eta^2} - 1, \end{aligned} \quad (16)$$

with

$$\begin{aligned} &\mathcal{L}_{\mathrm{f}}\left(C_1 + C_2\mathrm{e}^{-\eta} + C_3\mathrm{e}^{\eta}\right) = 0,\\ &\mathcal{L}_{\mathrm{g}}\left(C_4 + C_5\mathrm{e}^{-\eta} + C_6\mathrm{e}^{\eta}\right) = 0,\\ &\mathcal{L}_\theta\left(C_7\mathrm{e}^{-\eta} + C_8\mathrm{e}^{\eta}\right) = 0, \end{aligned} \quad (17)$$

where $C_i\,(i = 1 - 8)$ are the constants.

3.1. Zeroth-order deformation equations

Selecting the following nonlinear operators $\mathcal{N}_{\mathrm{f}}$, $\mathcal{N}_{\mathrm{g}}$, and $\mathcal{N}_\theta$:

$$\mathcal{N}_{\mathrm{f}}[f(\eta,\ p),\ g(\eta,\ p)] = \frac{\mathrm{d}^3 f(\eta,\ p)}{\mathrm{d}\eta^3} - \left(\frac{\mathrm{d}f(\eta,\ p)}{\mathrm{d}\eta}\right)^2 + (f(\eta,\ p) + g(\eta,\ p))\frac{\mathrm{d}^2 f(\eta,\ p)}{\mathrm{d}\eta^2}$$

$$+K_0\left[(f(\eta,\ p)+g(\eta,\ p))\frac{\mathrm{d}^4 f(\eta,\ p)}{\mathrm{d}\eta^4}\right.$$
$$+\left(\frac{\mathrm{d}^2 f(\eta,\ p)}{\mathrm{d}\eta^2}-\frac{\mathrm{d}^2 g(\eta,\ p)}{\mathrm{d}\eta^2}\right)\frac{\mathrm{d}^2 f(\eta,\ p)}{\mathrm{d}\eta^2}$$
$$\left.-2\left(\frac{\mathrm{d}f(\eta,\ p)}{\mathrm{d}\eta}+\frac{\mathrm{d}g(\eta,\ p)}{\mathrm{d}\eta}\right)\frac{\mathrm{d}^3 f(\eta,\ p)}{\mathrm{d}\eta^3}\right], \tag{18}$$

$$\mathcal{N}_{\mathrm{g}}[g(\eta,\ p),\ f(\eta,\ p)]$$
$$=\frac{\mathrm{d}^3 g(\eta,\ p)}{\mathrm{d}\eta^3}-\left(\frac{\mathrm{d}g(\eta,\ p)}{\mathrm{d}\eta}\right)^2$$
$$+(f(\eta,\ p)+g(\eta,\ p))\frac{\mathrm{d}^2 g(\eta,\ p)}{\mathrm{d}\eta^2}$$
$$+K_0\left[(f(\eta,\ p)+g(\eta,\ p))\frac{\mathrm{d}^4 g(\eta,\ p)}{\mathrm{d}\eta^4}\right.$$
$$+\left(\frac{\mathrm{d}^2 g(\eta,\ p)}{\mathrm{d}\eta^2}-\frac{\mathrm{d}^2 f(\eta,\ p)}{\mathrm{d}\eta^2}\right)\frac{\mathrm{d}^2 g(\eta,\ p)}{\mathrm{d}\eta^2}$$
$$\left.-2\left(\frac{\mathrm{d}f(\eta,\ p)}{\mathrm{d}\eta}+\frac{\mathrm{d}g(\eta,\ p)}{\mathrm{d}\eta}\right)\frac{\mathrm{d}^3 g(\eta,\ p)}{\mathrm{d}\eta^3}\right], \tag{19}$$

$$\mathcal{N}_{\theta}[\theta(\eta,\ p),\ f(\eta,\ p),\ g(\eta,\ p)]$$
$$=\frac{\mathrm{d}^2\theta(\eta,\ p)}{\mathrm{d}\eta^2}+Pr(f(\eta,\ p)+g(\eta,\ p))\frac{\mathrm{d}\theta(\eta,\ p)}{\mathrm{d}\eta}, \tag{20}$$

the zeroth-order problems are given by

$$(1-p)\,\mathcal{L}_{\mathrm{f}}\left[\bar{f}(\eta;p)-f_0(\eta)\right]$$
$$=p\hbar_f\mathcal{N}_{\mathrm{f}}\left[\bar{f}(\eta;p),\ \bar{g}(\eta;p)\right], \tag{21}$$

$$(1-p)\,\mathcal{L}_{\mathrm{g}}\left[\bar{g}(\eta;p)-g_0(\eta)\right]$$
$$=p\hbar_g\mathcal{N}_{\mathrm{g}}\left[\bar{g}(\eta;p),\ \bar{f}(\eta;p)\right], \tag{22}$$

$$(1-p)\,\mathcal{L}_{\theta}\left[\bar{\theta}(\eta;p)-\theta_0(\eta)\right]$$
$$=p\hbar_\theta\mathcal{N}_{\theta}\left[\bar{\theta}(\eta;\ p),\ \bar{f}(\eta;\ p),\ \bar{g}(\eta;\ p)\right], \tag{23}$$

$$\bar{f}(0;p)=0,\quad \bar{g}(0;p)=0,\quad \bar{f}'(0;p)=1,$$
$$\bar{g}'(0;p)=c,\quad \bar{\theta}(0;\ p)=-\gamma(1+\theta(0)),$$
$$\bar{f}'(\infty;p)=0,\quad \bar{g}'(\infty;p)=0,$$
$$\bar{g}''(\infty;p)=0,\quad \theta(\infty;p)=0, \tag{24}$$

where $p\in[0,\ 1]$ is an embedding parameter and $\hbar_f$, $\hbar_g$, and $\hbar_\theta$ are the non-zero auxiliary parameters. At $p=0$ and $p=1$ we have

$$\bar{f}(\eta;0)=f_0(\eta),\ \bar{g}(\eta;0)=g_0(\eta),\ \bar{\theta}(\eta;0)=\theta_0(\eta),$$
$$\bar{f}(\eta;1)=f(\eta),\ \bar{g}(\eta;1)=g(\eta),\ \bar{\theta}(\eta;1)=\theta(\eta). \tag{25}$$

Note that when p varies from 0 to 1, then $f(\eta,\ p)$, $g(\eta,\ p)$, and $\theta(\eta,\ p)$ change from initial guesses $f_0(\eta)$, $g_0(\eta)$, and $\theta_0(\eta)$ to the final solutions $f(\eta)$, $g(\eta)$, and $\theta(\eta)$. By using Taylor series we can write

$$f(\eta;p)=f_0(\eta)+\sum_{m=1}^{\infty}f_m(\eta)\,p^m, \tag{26}$$

$$g(\eta;p)=g_0(\eta)+\sum_{m=1}^{\infty}g_m(\eta)\,p^m, \tag{27}$$

$$\theta(\eta;p)=\theta_0(\eta)+\sum_{m=1}^{\infty}\theta_m(\eta)\,p^m, \tag{28}$$

$$f_m(\eta)=\frac{1}{m!}\frac{\partial^m f(\eta;p)}{\partial\eta^m},\quad g_m(\eta)=\frac{1}{m!}\frac{\partial^m g(\eta;p)}{\partial\eta^m},$$
$$\theta_m(\eta)=\frac{1}{m!}\frac{\partial^m\theta(\eta;p)}{\partial\eta^m}. \tag{29}$$

The convergence of the above series is strongly dependent on $\hbar_f$, $\hbar_g$, and $\hbar_\theta$. Suppose that $\hbar_f$, $\hbar_g$, and $\hbar_\theta$ are chosen in such a way that the series solutions converge at $p=1$. Then we have

$$f(\eta;p)=f_0(\eta)+\sum_{m=1}^{\infty}f_m(\eta), \tag{30}$$

$$g(\eta;p)=g_0(\eta)+\sum_{m=1}^{\infty}g_m(\eta), \tag{31}$$

$$\theta(\eta;p)=\theta_0(\eta)+\sum_{m=1}^{\infty}\theta_m(\eta). \tag{32}$$

3.2. *m*th-order deformation equations

The *m*th-order deformation equations are obtained by differentiating Eqs. (21)–(23) m times with respect to p, then putting $p=0$ we get

$$\mathcal{L}_{\mathrm{f}}[f_m(\eta)-\chi_m f_{m-1}(\eta)]=\hbar_f\mathcal{R}_{\mathrm{f}}^m(\eta), \tag{33}$$

$$\mathcal{L}_{\mathrm{g}}[g_m(\eta)-\chi_m g_{m-1}(\eta)]=\hbar_g\mathcal{R}_g^m(\eta), \tag{34}$$

$$\mathcal{L}_{\theta}[\theta_m(\eta)-\chi_m\theta_{m-1}(\eta)]=\hbar_\theta\mathcal{R}_\theta^m(\eta), \tag{35}$$

$$f_m(0)=f_m'(0)=f_m'(\infty)=f_m''(\infty)=0,$$
$$g_m(0)=g_m'(0)=g_m'(\infty)=g_m''(\infty)=0,$$
$$\theta_{\mathrm{m}}'(0)+\gamma\theta_m(0)=0,\ \theta(\infty)=0, \tag{36}$$

$$\mathcal{R}_{\mathrm{f}}^m(\eta)=f_{m-1}'''(\eta)-\sum_{k=0}^{m-1}f_{m-1-k}'f_k'$$
$$+\sum_{k=0}^{m-1}[f_{m-1-k}+g_{m-1-k}]f_k''$$
$$+K_0\sum_{k=0}^{m-1}\left[(f_{m-1-k}+g_{m-1-k})f_k^{(iv)}\right.$$
$$+\left(f_{\mathrm{m-1-k}}''-g_{m-1-k}''\right)f_k''$$
$$\left.-2\left(f_{m-1-k}'+g_{m-1-k}'\right)f_k'''\right], \tag{37}$$

$$\mathcal{R}_{\mathrm{g}}^m(\eta)=g_{m-1}'''(\eta)-\sum_{k=0}^{m-1}g_{m-1-k}'g_k'$$
$$+\sum_{k=0}^{m-1}[f_{m-1-k}+g_{m-1-k}]g_k''$$
$$+K_0\sum_{k=0}^{m-1}\left[(f_{m-1-k}+g_{m-1-k})g_k^{(iv)}\right.$$
$$+\left(g_{m-1-k}''-f_{m-1-k}''\right)g_k''$$
$$\left.-2\left(f_{m-1-k}'+g_{m-1-k}'\right)g_k'''\right], \tag{38}$$

$$\mathcal{R}_\theta^m(\eta)=\theta_{m-1}''(\eta)+Pr\sum_{k=0}^{m-1}[f_{m-1-k}+g_{m-1-k}]\theta_k', \tag{39}$$

$$\chi_m = \begin{cases} 1, & m \leq 1, \\ 0, & m > 1. \end{cases} \tag{40}$$

Denoting $f_m^*(\eta)$, $g_m^*(\eta)$, and $\theta_m^*(\eta)$ as the special solutions, the final solutions are

$$f_m(\eta) = f_m^*(\eta) + C_1 + C_2 e^{-\eta} + C_3 e^{\eta}, \tag{41}$$

$$g_m(\eta) = g_m^*(\eta) + C_4 + C_5 e^{-\eta} + C_6 e^{\eta}, \tag{42}$$

$$\theta_m(\eta) = \theta_m^*(\eta) + C_7 e^{-\eta} + C_8 e^{\eta}. \tag{43}$$

3.3. Convergence of the solution

Here we are interested in discussing the convergence of the derived series solutions. The convergence of solutions for the nonlinear differential equation is vital and essential every time. In the present case, we have utilized an efficient analytic technique namely the homotopy analysis method (HAM)[20–25] to construct the analytic solutions for the highly nonlinear and coupled differential system. It is seen that the convergence of Eqs. (40)–(42) strongly depends upon non-zero auxiliary parameters ($\hbar_f$, $\hbar_g$, and $\hbar_\theta$) and these non-zero auxiliary parameters have a definite role in adjusting and controlling the convergence of the obtained solutions. In order to find the admissible values for ($\hbar_f$, $\hbar_g$ and $\hbar_\theta$), the $\hbar$ curves are displayed for the 15th order of approximation in Figs. 1 and 2. It is noted that the convergence range for admissible values of ($\hbar_f$, $\hbar_g$ and $\hbar_\theta$) is $-2.0 \leq (\hbar_f, \hbar_g, \hbar_\theta) \leq -0.4$. Thus, by selecting the values of ($\hbar_f$, $\hbar_g$, and $\hbar_\theta$) from this range we get the correct and convergent solutions for the velocity and temperature profiles up to the 6th decimal place. Moreover, we have also constructed the graphs of residual errors as shown in Figs. 3–5. From these plots it is observed that the error in our computation is very negligible. Thus these plots ensure the validity of the whole analysis.

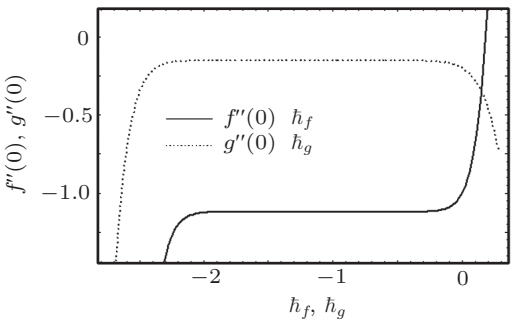


Fig. 1. $\hbar$ curves of f and g. $c = 0.2$, $K_0 = 0.1$, $Pr = 1.0$, $\gamma = 0.1$.

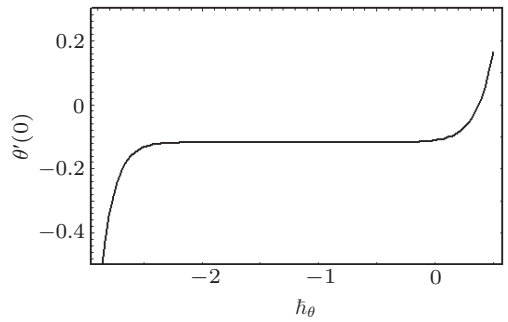


Fig. 2. $\hbar$ curve of θ. $c = 0.5$, $K_0 = 0.1$, $Pr = 1.0$, $\gamma = 0.1$.

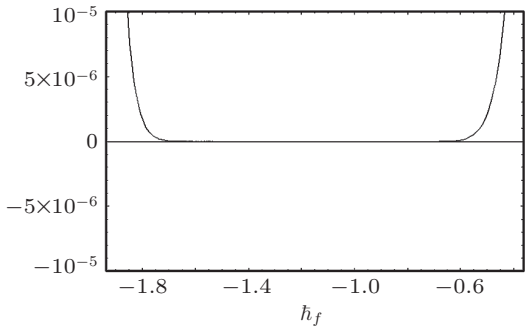


Fig. 3. $\hbar$ curve for residual error in $f(\eta)$.

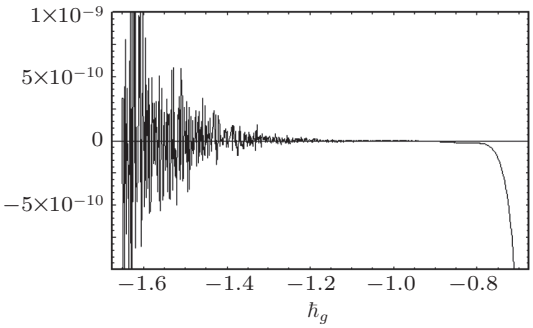


Fig. 4. $\hbar$ curve for residual error in $g(\eta)$.

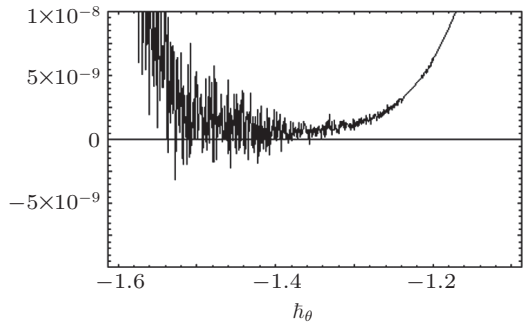


Fig. 5. $\hbar$ curve for residual error in $\theta(\eta)$.

Table 1. Convergence of the HAM solutions for different orders of approximation when $c = 0.2$, $K_0 = \gamma = 0.1$, $Pr = 1.0$.

Order of approximation	$-f''(0)$	$-g''(0)$	$-\theta'(0)$
1	1.085333	0.1744000	0.1140740
2	1.110392	0.1620039	0.1158053
5	1.120768	0.1526537	0.1179168
10	1.121067	0.1518856	0.1185831
15	1.121067	0.1518809	0.1186677
20	1.121067	0.1518810	0.1186796
25	1.121067	0.1518810	0.1186813
30	1.121067	0.1518810	0.1186816
40	1.121067	0.1518810	0.1186816
50	1.121067	0.1518810	0.1186816

Table 1 confirms the order of approximations necessary for a convergent solution. This Table concludes that the 10th order of approximations is sufficient for f , the 20th order of approximation is sufficient for g and the 30th order of approximations is sufficient for θ. Table 2 provides a comparative study for viscous flow. It is found that the present HAM solution has a good agreement with the limiting exact and HPM solutions provided in Ref. [16].

Table 2. Illustrating the variations of $-f''(0)$ and $-g''(0)$ with c when $K_0 = 0$ using HAM,[16] and an exact solution.[16]

c	$-f''(0)$			$-g''(0)$		
	HAM	HPM[16]	Exact[16]	HAM	HPM[16]	Exact[16]
0.0	1.000000	1.000000	1.000000	0.000000	0.000000	0.000000
0.1	1.020259	1.017027	1.020259	0.066847	0.073099	0.066847
0.2	1.039495	1.034587	1.039495	0.148736	0.158231	0.148736
0.3	1.057954	1.052470	1.057954	0.243359	0.254347	0.243359
0.4	1.075788	1.070529	1.075788	0.349208	0.360599	0.349208
0.5	1.093095	1.088662	1.093095	0.465204	0.476290	0.465204
0.6	1.109946	1.106797	1.109946	0.590528	0.600833	0.590528
0.7	1.126397	1.124882	1.126397	0.724531	0.733730	0.724531
0.8	1.142488	1.142879	1.142488	0.866682	0.874551	0.866682
0.9	1.158253	1.160762	1.158253	1.016538	1.022922	1.016538
1.0	1.173720	1.178511	1.173720	1.173720	1.178511	1.173720

4. Discussion

This section highlights the effects of different parameters on the velocity components $f'(\eta)$, $g'(\eta)$ and the temperature $\theta(\eta)$. Therefore, we displayed the Figs. 6–12. The variations of parameter c are plotted in the Figs. 6 and 7. It is clear from Fig. 6 that the velocity component f' decreases when c increases, whereas g' increases with an increase in c (see Fig. 7). Physically, when c increases from zero, the velocity component in the original stretching direction f' decreases and the lateral surface begins to move in the y direction and thus the velocity component g' increases. The variations of K_0 on f' and g' are portrayed in the Figs. 8 and 9. These figures indicate that f', g' and their associated boundary layer are decreasing functions of K_0. Figure 10 shows the variation of Newtonian heating parameter γ. We concluded from this figure that the temperature profile increases with the increase in γ. The wall temperature increases with the increase in γ. It is expected since the Newtonian heating condition becomes the prescribed wall temperature when γ goes to infinity. It is also noted that the fluid temperature is zero when γ is zero. From the physical point of view, one can see that when γ increases, the Newtonian heating parameter increases. That enhancement in the Newtonian heating parameter leads to an increase in the temperature. Figure 11 shows that when we increase the viscoelastic parameter K_0, the temperature profile increases. Variations of Prandtl number Pr are shown in Fig. 12. It is seen that an increase in Prandtl number Pr shows a decrease in the temperature of the fluid and the thermal boundary layer thickness. Physically, an increase in the Prandtl number leads to a decrease in the thermal diffusivity and so the temperature and thermal boundary layer thickness decrease. Table 3 shows that with the increase of ratio parameter c and Prandtl number Pr, the local Nusselt number increases, while with an increase of viscoelastic parameter K_0, the local Nusselt number decreases.

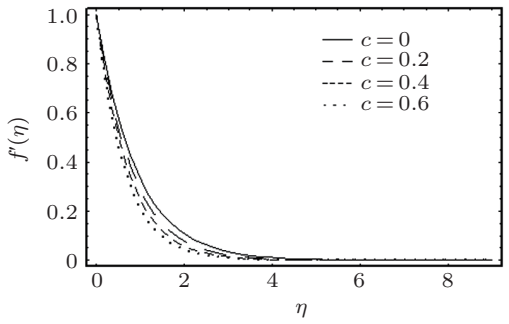


Fig. 6. Influence of c on $f'(\eta)$. $K_0 = 0.1$ and $Pr = 1.0$.

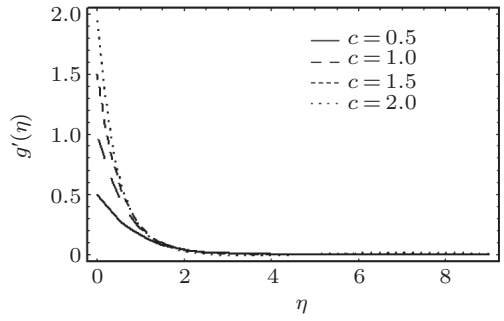


Fig. 7. Influence of c on $g'(\eta)$. $K_0 = 0.1$ and $Pr = 1.0$.

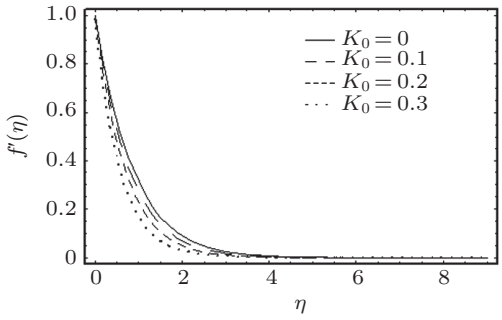


Fig. 8. Influence of K_0 on $f'(\eta)$. $c = 0.5$ and $Pr = 1.0$.

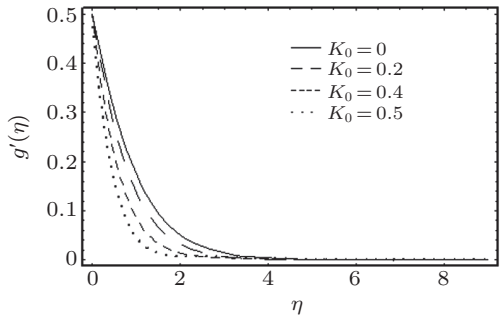


Fig. 9. Influence of K_0 on $g'(\eta)$. $c = 0.5$ and $Pr = 1.0$.

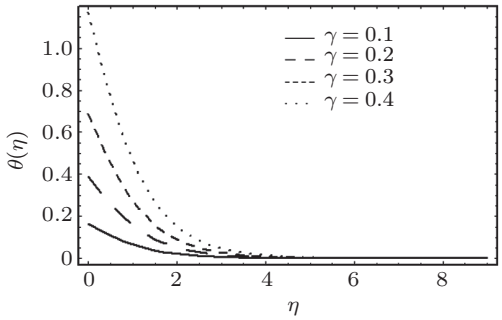


Fig. 10. Influence of γ on $\theta(\eta)$. $Pr = 1.0$, $K_0 = 0.1$, and $c = 0.2$.

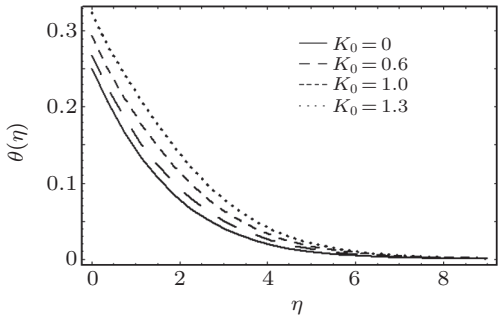


Fig. 11. Influence of K_0 on $\theta(\eta)$. $c = 1.0$, $Pr = 0.2$, and $\gamma = 0.1$.

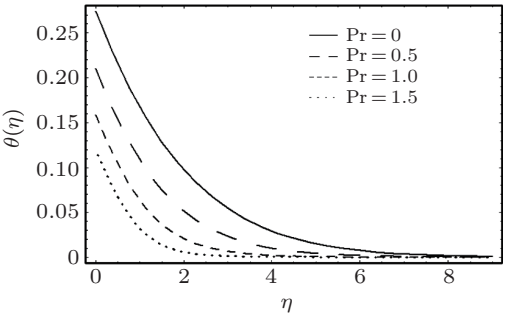


Fig. 12. Influence of Pr on $\theta(\eta)$. $c = 0.5$ and $K_0 = \gamma = 0.1$.

Table 3. Values of the local Nusselt number $Re_x^{-1/2}\, Nu_x$ for some values of c, K_0, Pr, and $\gamma = 0.1$.

c	K_0	Pr	$\gamma[1+1/\theta(0)]$
0.0	0.1	1.0	0.570832
0.5			0.711118
1.0			0.807171
0.5	0.0		0.735331
	0.1		0.711118
	0.2		0.678014
	0.1	1.0	0.711118
		1.3	0.848465
		1.5	0.931612

5. Concluding remarks

Three dimensional flow of viscoelastic fluid over a stretching sheet with Newtonian heating is examined. The main results can be summarized as follows.

(i) The behaviors of the ratio parameter on the velocity components f' and g' are the opposite.

(ii) There is a decrease in the velocity boundary layer when the viscoelastic parameter increases.

(iii) Prandtl number leads to a decrease in the thermal boundary layer thickness.

References

[1] Jamil M, Rauf A, Fetecau C and Khan N A 2011 *Comm. Nonlinear Sci. Numer. Simul.* **16** 1959

[2] Fetecau C, Mahmood A and Jamil M 2010 *J. Non-Newtonian Fluid Mech.* **165** 350

[3] Hayat T, Alsaedi A and Bhattacharyya K 2013 *Chin. Phys. B* **22** 024702

[4] Kang J, Fu C and Tan W 2011 *J. Non-Newtonian Fluid Mech.* **166** 93

[5] Salem A M and Fathy R 2012 *Chin. Phys. B* **21** 054701

[6] Haitao Q and Mingyu X 2007 *Mech. Research Comm.* **34** 210

[7] Hayat T, Awais M and Sajid M 2011 *Int. J. Mod. Phys. B* **25** 2863

[8] Hayat T, Awais M and Obaidat S 2012 *Comm. Nonlinear Sci. Numer. Simul.* **17** 699

[9] Bhattacharyya K, Mukhopadhyay S and Layek G C 2011 *Chin. Phys. Lett.* **28** 094702

[10] Hayat T, Safdar A, Awais M and Mesloub S 2012 *Int. J. Heat Mass Trans.* **55** 2129

[11] Bhattacharyya K, Hayat T and Alsaedi A 2013 *Chin. Phys. B* **22** 024702

[12] Eerdunbuhe and Temuerchaolu 2012 *Chin. Phys. B* **21** 035201

[13] Wang S and Tan W 2011 *Int. J. Heat Fluid Flow* **32** 88

[14] Mukhopadhyay S 2010 *Chin. Phys. Lett.* **27** 124401

[15] Hayat T, Naz R, Asghar S and Mesloub S 2012 *Nuclear Engin. Design* **243** 1

[16] Li B, Xu Z W, Zhao Z G 2009 *Acta Phys. Sin.* **58** 5750 (in Chinese)

[17] Crane L J 1970 *Z. Angew. Math. Phys.* **21** 645

[18] Mukhopadhyay S 2009 *Int. J. Heat Mass Trans.* **52** 3261

[19] Ishak A, Nazar R and Pop I 2007 *Chin. Phys. Lett.* **24** 2274

[20] Bhattacharyya K 2013 *Chin. Phys. B* **22** 074705

[21] Hayat T, Awais M, Asghar S and Hendi A A 2011 *ASME J. Fluid Eng.* **133** 061201

[22] Ariel P D 2007 *Comp. Math. App.* **54** 920

[23] Singh A K 2005 *Int. Comm. Heat Mass Trans.* **32** 1420

[24] Hayat T, Awais M and Obaidat S 2012 *ASME J. Heat Transfer* **134** 044503

[25] Merkin J H 1994 *a J. Appl. Math. Phys.* **45** 258

[26] Liao S J 2003 Beyond Perturbation Introduction to Homotopy Analysis Method. (Boca Raton: Chapman & Hall/CRC Press)

[27] Rashidi M M, Mohimanian pour S A and Abbasbandy S 2011 *Comm. Nonlinear Sci. Numer. Simulat.* **16** 1874

[28] Keimanesh M, Rashidi M M, Chamkha A J and Jafari R 2011 *Computers Mathematics Appl.* **62** 2871

[29] Qayyum A, Awais M, Alsaedi A and Hayat T 2012 *Chin. Phys. Lett.* **29** 034701

[30] Hayat T and Awais M 2011 *Int. J. Numer. Methods Fluids* **66** 875

[31] Turkyilmazoglu M 2013 *Appl. Math. Modelling* **37** 7539

[32] Sweilam N H and Khader M M 2011 *World Applied Sci. J.* **3** 1

[33] Khader M M 2013 *J. Nanotech. Adv. Mater.* **1** 59

[34] Khadera M M, Kumar S and Abbasbandy S 2013 *Chin. Phys. B* **22** 110201

[35] Abbasbandy S 2007 *Phys. Lett. A* **361** 478